Carbohydrate Polymers 85 (2011) 584–591

Contents lists available at ScienceDirect

Carbohydrate Polymers

journal homepage: www.elsevier.com/locate/carbpol

β-Chitin hydrogel/nano hydroxyapatite composite scaffolds for tissue engineering applications

P.T. Sudheesh Kumar[a], Sowmya Srinivasan[a], Vinoth-Kumar Lakshmanan[a], H. Tamura[b], S.V. Nair[a], R. Jayakumar[a,*]

[a] Amrita Centre for Nanosciences and Molecular Medicine, Amrita Institute of Medical Sciences and Research Centre, Amrita Vishwa Vidyapeetham University, Kochi 682041, India
[b] Faculty of Chemistry, Materials and Bioengineering, Kansai University, Osaka 564-8680, Japan

ARTICLE INFO

Article history:
Received 3 February 2011
Received in revised form 8 March 2011
Accepted 10 March 2011
Available online 17 March 2011

Keywords:
β-Chitin
Hydroxyapatite
Nanocomposite
Biomineralization
Scaffold
Cell viability
Tissue engineering

ABSTRACT

β-Chitin hydrogel/nano hydroxyapatite (nHAp) nanocomposite scaffolds were prepared by freeze-drying approach from the mixture of β-chitin hydrogel and nHAp in different concentrations such as 0.5 and 1%, respectively. The prepared nHAp and nanocomposite scaffolds were characterized using various modalities. Porosity, swelling ability, *in vitro* degradation, protein adsorption and biomineralization of the prepared composite scaffolds were evaluated. The composite scaffolds were found to have 70–80% porosity with well defined interconnected porous structure. The scaffolds also showed a swelling ratio of 15–20, controlled biodegradation of about 30–40% with enhanced protein adsorption. In addition, the cell viability, attachment and proliferation using MG 63, Vero, NIH3T3 and nHDF cells confirmed the cytocompatibility nature of the nanocomposite scaffolds with well improved cell attachment and proliferation. All these results essentially signify that this material can be a potential candidate for bone and wound tissue engineering applications.

1. Introduction

Chitin is a natural biopolymer found in the shells of crustaceans. It is the second most abundant polymer on earth after cellulose. Chitin contains D-glucosamine and N-acetyl-D-glucosamine units. The monomers are inter-connected by β-glycosidic linkages (Rudall & Kenchington, 1973). There are different polymorphic forms of chitin namely α, and β. Crabs and shrimps are the main source of α-chitin, whereas β-chitin is isolated from squid pen and γ-chitin from loligo (Jang, Kong, Jeong, Lee, & Nah, 2004; Rashidova et al., 2004). They differ in the arrangement of polymeric chains. In the case of α-chitin, the polymer chains run antiparallel to each other whereas they are arranged parallel in the case of β-chitin (Blackwell, 1969). Chitin has numerous advantages such as biocompatibility, biodegradability, wound healing ability, etc. (Jayakumar, Prabaharan, Sudheesh, Nair, & Tamura, 2011; Muzzarelli, 2009; Nagahama et al., 2008; Sudheesh et al., 2010). Literature has reported that chitin possesses the capability to form composites with polymers as well as ceramics (Muzzarelli, 2009; Sudheesh et al., 2010).

β-Chitin has been employed for various biomedical applications like wound dressing, as scaffolds for tissue engineering applications, etc. (Jayakumar et al., 2011; Maeda, Jayakumar, Nagahama, Furuike, & Tamura, 2008; Peesan, Rujiravanit, & Supaphol, 2003; Sudheesh et al., 2010; Sugiyama, Boisset, & Hashimoto, 1999). This material enhances the bioactivity and promotes tissue regeneration. The degradation product is D-glucosamine which further enhances the deposition of collagen in the presence of a wound. Intermolecular interactions in β-chitin are weaker than in α-chitin. This is because of the polymer chain arrangement and thus enabling β-chitin to be more susceptible to dissolution in numerous solvents. Few reports exploited the composite forming ability of the β-chitin with other polymers and ceramics. β-Chitin forms hydrogen bonds with other polymers and ceramics and with this capability β-chitin holds other polymers and ceramics intact to serve as a better composite. This ultimately results in a more reactive and versatile β-chitin (Lavall, Assis, & Filho, 2007; Madhumathi et al., 2009; Maeda et al., 2008; Saito, Okano, Gaill, Chanzy, & Putaux, 2000).

Hydroxyapatite [(HAp), $Ca_{10}(PO_4)_6(OH)_2$]; is a major inorganic ceramic material and an essential component of the bone. It has numerous exceptional properties like bioactivity, osteoconductivity, osteoinductivity, slow biodegradability, non toxicity and easy synthesizability (Chai, Nissan, Pyke, & Evans, 1995; Heise, Osborn, & Duwe, 1990). HAp is being used for various applications like bone

* Corresponding author. Tel.: +91 484 2801234; fax: +91 484 2802020.
E-mail addresses: rjayakumar@aims.amrita.edu, jayakumar77@yahoo.com (R. Jayakumar).

0144-8617/$ – see front matter © 2011 Elsevier Ltd. All rights reserved.
doi:10.1016/j.carbpol.2011.03.018

tissue engineering (Muzzarelli, 2011; Peter et al., 2010), dental filling material, etc. (Labella, Bradena, & Deb, 1994). nHAp offers high surface area to volume ratio and a small concentration is sufficient to enhance bioactivity and osseointegration (Liuyun, Yubao, & Chengdong, 2009; Peter et al., 2010). Many works have been reported on composite materials containing nHAp in combination with natural and synthetic biopolymers for tissue engineering applications (Bonfield, Grynpas, Tully, & Bowman, 1981; Verheyen, Dewijn, van Blitterswijk, & de Groot, 1992; Wang et al., 2007; Wang, Li, Wei, & Groot, 2002).

Recently hydrogel based scaffolds are gaining attention in the field of tissue engineering (Nguyen and West, 2002; Tan and Marra, 2010). The hydrogel scaffolds have an inherent ability to swell in aqueous medium thus permitting the transportation of enzymes and nutrients to and through the scaffolds (Gkioni, Leeuwenburgh, Douglas, Mikos, and Jansen (2010); Tamura, Furuike, Nair, & Jayakumar, 2011). In this work we synthesized β-chitin hydrogel/nHAp nanocomposite scaffolds by incorporating nHAp into β-chitin hydrogel for tissue engineering applications. The synthesized composite scaffolds were characterized and bioactivity studies were performed.

2. Materials and methods

2.1. Materials

β-Chitin (Degree of Acetylation-72.4%) was purchased from Koyo Chemical Co. Ltd., Japan. $CaCl_2$ and methanol were purchased from Qualigens, India. Calcium nitrate, ammonia and ammonium dihydrogen orthophosphate were obtained from Merck. Glutaraldehyde and hen lysozyme were purchased from Fluka. DAPI, Alamar Blue, Trypsin–EDTA and Fetal Bovine Serum (FBS) were obtained from Gibco, Invitrogen Corporation. Minimum essential medium (MEM) was purchased from Sigma–Aldrich Company. The Vero (epithelial cells), MG 63 (osteosarcoma cells) and NIH3T3 (fibroblast cells) were provided by National Center for Cell Sciences, Pune, India. HDF (normal human dermal fibroblast) cell was purchased from Promocell, Germany. The chemicals were used without further purification.

2.2. Methods

2.2.1. Preparation of β-chitin hydrogel

β-Chitin hydrogel was prepared according to the literature (Maeda et al., 2008; Sudheesh et al., 2010; Tamura, Nagahama, & Tokura, 2006). β-Chitin powder was added to saturated $CaCl_2$/methanol solvent and stirred vigorously for 48 h at room temperature. On attaining a transparent β-chitin solution, the solution was filtered to remove the undissolved traces. To this solution excess water was added and stirred vigorously for 2 h in order to obtain β-chitin hydrogel. The hydrogel was allowed to stand for 24 h and filtered using Whatman filter paper. The obtained hydrogel was dialyzed against distilled water for two days to obtain pure β-chitin hydrogel.

2.2.2. Preparation of nano hydroxyapatite (nHAp)

Nano hydroxyapatite (nHAp) was synthesized in aqueous solution as reported earlier (Wang et al., 2002). The pH value of the solutions of $Ca(NO_3)_2$ and $(NH_4)H_2PO_4$ was adjusted to more than 10 with ammonia. Then they were mixed in a stoichiometric ratio of Ca to P (1.67). On completion of the reaction, the precipitate was rinsed for several times with distilled water until the pH value dropped to 7. Following which the precipitate was dried at 80 °C, calcined at 400 °C and sintered at 800 °C to obtain crystalline HAp. The HAp nanosuspension was prepared by bath sonication of HAp in distilled water for 20 min.

2.2.3. Preparation of β-chitin hydrogel/nHAp composite scaffolds

The prepared HAp nanosuspension was mixed with β-chitin hydrogel at concentrations of 0.5 and 1% (w/w). The whole system was vigorously stirred for 30 min to get a homogenized mixture and the obtained mixture was further freezed at −20 °C and lyophilized to get microporous nanocomposite scaffolds.

2.3. Characterization

The particle size and size distribution of nHAp were analyzed using dynamic light scattering measurements (DLS-ZP/Particle Sizer Nicomp™ 380 ZLS, particle sizing system). Composite scaffolds and nHAp were characterized using FT-IR spectroscopy (Spectrophotometer Perkin-Elmer RX1). Composite scaffolds and nHAp were ground and mixed thoroughly with potassium bromide and pelletized. The IR spectra were analyzed in the range of 400–4000 cm^{-1}. The structural morphology of the nanocomposite scaffolds and nHAp was examined using scanning electron microscope (JEOL, JSM-6490LA, JAPAN). Nanocomposite scaffold samples were prepared by taking a thin section of the scaffold using a razor blade. The sections were then platinum sputter coated in vacuum (JEOL, JFC-1600, Japan), and examined using scanning electron microscope. XRD pattern of the nanocomposite scaffolds and nHAp was analyzed at room temperature using a Panalytical diffractometer (XPERT PRO powder) (Cu Kα radiations) operating at a voltage of 40 kV. XRD was taken at a 2θ angle range of 5–70° and the process parameters were: scan step size 0.02 and scan step time 0.05 s. Thermogravimetric analysis of the scaffolds and nHAp was carried out using TG/DTA instrument (SII TG-DTA6200) at a temperature range of 25–500 °C.

2.4. Porosity studies

The porosity of the prepared nanocomposite scaffolds was estimated using the reported method (Liuyun et al., 2009). Briefly, the scaffolds were immersed in absolute ethanol until saturated. The weights of the scaffolds before and after immersion in alcohol were noted. The porosity was calculated using the formula,

$$P = \frac{W_2 - W_1}{\rho V_1}$$

where W_1 and W_2 indicate the weight of the scaffolds before and after immersing, respectively, and V_1 is the volume before immersing, ρ is a constant density of ethanol. All samples were triplicated in the experiment.

2.5. Swelling studies

Nanocomposite scaffolds were cut into small pieces having equal weights and immersed in phosphate buffered saline (PBS, pH 7.4, 37 °C). The scaffolds were removed at different time periods and water on the surface was gently blotted on a filter paper and weighed (W_d).

$$DS = \frac{W_w - W_d}{W_d}$$

where DS is the degree of swelling and W_w & W_d are the wet and dry weights of the scaffolds, respectively.

2.6. In vitro degradation studies

The degradation of the scaffolds was studied in PBS (pH 7.4) medium containing lysozyme at 37 °C. Scaffolds were equally weighed and immersed in lysozyme (10,000 U/ml) containing medium and incubated at 37 °C for 28 days. Initial weight of the scaffold was noted as W_i. The scaffolds were taken out from

the medium at 7, 14, 21 and 28 days and washed in deionised water to remove ions adsorbed on surface. The scaffolds were then freeze-dried and weighed. The final weight was noted as W_t. The degradation was calculated using the formula

$$\text{degradation}(\%) = \frac{W_i - W_t}{W_i} \times 100$$

2.7. In vitro biomineralization studies

The scaffolds having equal weight and shape were immersed in 1× simulated body fluid (SBF) (Kokubo & Takadama, 2006) solution and incubated at 37 °C in closed falcon tubes up to 28 days. After the specified time intervals, the scaffolds were removed from SBF solution and washed thrice with deionised water to remove adsorbed minerals. Finally the scaffolds were freeze-dried, sectioned and viewed using SEM for mineralization. The formation of minerals was confirmed by analyzing the FT-IR and XRD spectra of the scaffolds which were treated with SBF solution.

2.8. Protein adsorption study

Nanocomposite scaffolds having equal weights were taken and placed into a well plate preoccupied with MEM (supplemented with 10% FBS) culture media and incubated at 37 °C. After 2, 4 & 6 h of incubation, the scaffolds were rinsed with PBS solution thrice to remove the proteins and ions which were not adsorbed on the surface. Total protein concentration was quantified using bicinchoninic acid (BCA) assay (Binulal et al., 2010). The principle of BCA assay is based on the reduction of Cu^{2+} to Cu^{1+}. The amount of reduction is proportional to the concentration of protein present. BCA reagent was added to each well and incubated for 30 min with the extract at 37 °C and the absorbance was read at a wavelength of 562 nm. Scaffolds incubated in serum free medium were used as blank.

2.9. Cell viability study

Cell viability of the prepared β-chitin hydrogel/nHAp composite scaffolds was evaluated by indirect cytotoxicity test using Alamar Blue assay (Binulal et al., 2010). The cytotoxicity test of composite scaffolds was done according to ISO 10993-5. The cytotoxic effect of β-chitin control and β-chitin with different concentrations of nHAp was evaluated on human osteosarcoma (MG63), monkey epithelial (Vero), mouse fibroblast (NIH3T3) and human dermal fibroblast (HDF) cell lines. MG63, Vero, NIH3T3, and HDF cells were cultured in MEM supplemented with 10% FBS, 50 IU/ml penicillin and 50 μg ml^{-1} streptomycin (Invitrogen, CA, USA). Scaffolds were sterilized by ethylene oxide gas and extraction ratio was 0.2 g/ml (sample/medium). The sterilized samples were incubated in serum containing media for 24 h and 48 h at 37 °C. 100 μl of the sample extract was taken for the viability test. The cells were seeded onto a 96 well plate at a seeding density 1×10^4 cells/well and incubated overnight at 37 °C. The media was replaced with the extract and further incubated for 24 h and 48 h. After the incubation period, the extract was replaced with fresh media containing Alamar Blue (Invitrogen, USA) solution and again kept for incubation. After 4 h of incubation, the absorbance was measured at 570 nm with 620 nm set as the reference wavelength using a microplate spectrophotometer (Biotek PowerWave XS, USA).

2.10. Cell attachment and proliferation studies

The attachment and spreading nature of MG63, Vero, NIH3T3, and HDF cells on the composite scaffolds was evaluated using SEM and DAPI staining. Cells were seeded drop wise onto the top of the scaffolds (1×10^5 cells/scaffold), which fully absorbed the media, allowing cells to distribute throughout the scaffolds and incubation at 37 °C for 12 and 72 h, respectively. After 12 and 72 h of incubation, cell seeded composite scaffolds were fixed with 2.5% glutaraldehyde, rinsed with PBS and dehydrated using graded series of ethanol (20–100%). The samples were coated with platinum and examined under SEM. DAPI or 4′,6-diamidino-2-phenylindole is a fluorescent stain that is using for the nuclear staining of cells. For DAPI staining the cell seeded scaffolds were fixed with 4% paraformaldehyde for 20 min, permeabilised with 0.5% Triton X-100 (in PBS) for 5 min. Then the scaffolds were treated with 1% FBS, washed with PBS and stained with 50 μl of DAPI (1:30 dilution with PBS) and incubated in dark for 3 min. The scaffolds were then washed with PBS and viewed under fluorescent microscope (Olympus-BX-51).

3. Results and discussion

3.1. Characterization of nHAp and composite scaffolds

It was clear from the DLS data that the particles were in a polydispersed state; having size in the range of 50–120 nm which was further confirmed by SEM analysis.

FT-IR spectrum of the synthesized nHAp particles having peaks at 565, 602 and 3570 cm^{-1} are the characteristic peaks of nHAp (Wang et al., 2002). The peaks at 565 and 602 cm^{-1} correspond to stretching vibrations of phosphate group present in the nHAp and peak at 3570 cm^{-1} corresponds to stretching vibration of OH group present in the nHAp (Wang et al., 2002).

XRD spectrum of nHAp has been taken and compared with the standard XRD spectrum of nHAp and the spectrum exactly matched the standard spectrum (JCPDS File number: 09-0432) (refer Supplementary Data).

Fig. 1 shows the SEM image of control (A) and composite scaffolds (B & C). The composite scaffolds appeared as porous nature. The porosity of the scaffolds was decreased with the increase in the concentration of nHAp. The nHAp particles act as fillers making the polymer chains intact and hence cause a reduction in the porosity (Peter et al., 2010). In the case of control, the pores were arranged uniformly and interconnected with walls of the scaffold. nHAp incorporated scaffolds were found to have a compact nature. This will further help in the enhancement of biomineralization ability and provide suitable cell attachment as well.

Fig. 1D shows the FT-IR spectra of nHAp, β-chitin control and β-chitin hydrogel/nHAp composite scaffolds. In the spectra (a) is β-chitin control; (b) is nHAp control; (c) is β-chitin + 0.5% nHAp and (d) is β-chitin + 1% nHAp. In the case of β-chitin control (a) the peak at 1650 is due to the intracellular hydrogen bonding between the carbonyl groups of amide I and the amide II (Rudall & Kenchington, 1973). From spectrum c & d it was found that incorporation of nHAp into β-chitin hydrogel caused the broadening of the peak at 3450 cm^{-1} (characteristic of β-chitin); which was due to the intermolecular hydrogen bonding between $-NH_2$ group of β-chitin and –OH group of nHAp. The characteristic peaks of HAp were present in the spectrum of composite scaffolds. The intensity of peaks at 565 and 602 cm^{-1} was less in β-chitin + 0.5% nHAp scaffold; because the concentration of nHAp is less. But in β-chitin + 1% nHAp scaffold, the peaks have resolved and intensity was also increased.

Fig. 1E shows the XRD spectra of nHAp (a) β-chitin (b) and β-chitin hydrogel/nHAp composite scaffolds (c & d). The peaks of the synthesized nHAp particles matched the characteristic XRD spectrum of HAp (JCPDS File No. 09-0432). The distinctive peaks of β-chitin and nHAp can be noticed in (c & d). Peaks at 10° and 20° are characteristic of β-chitin; which are present in the spectrum (b). The peaks of β-chitin and nHAp were present in both (c & d)

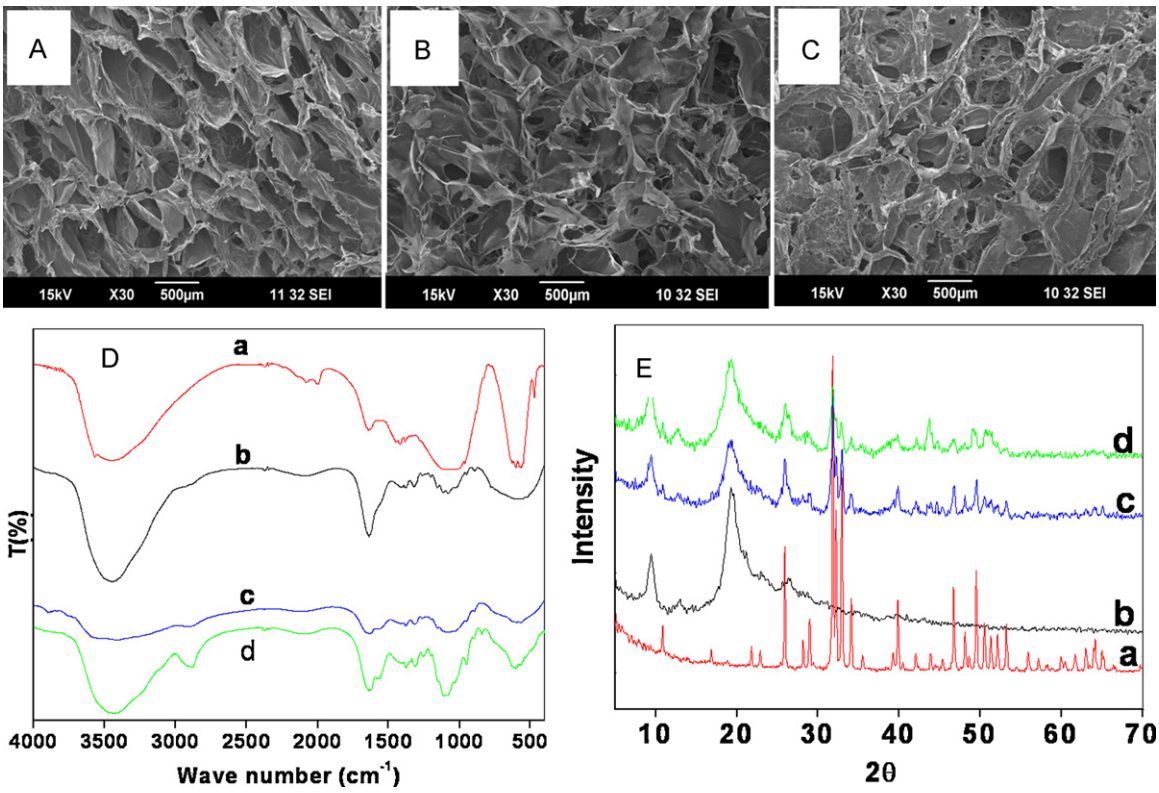

Fig. 1. (A) SEM image of β-chitin control scaffold. (B) β-Chitin + 0.5% nHAp composite scaffold. (C) β-Chitin + 1% nHAp. (D) FT-IR spectra of composite scaffolds (a) nHAp control, (b) β-chitin control, (c) β-chitin + 0.5% nHAp and (d) β-chitin + 1% nHAp. (E) XRD spectra of composite scaffolds (a) nHAp control, (b) β-chitin control, (c) β-chitin + 0.5% nHAp and (d) β-chitin + 1% nHAp.

the spectrums. In 0.5% nHAp incorporated scaffolds, the intensity of the peaks was less and at higher concentration of nHAp the intensity was increased. The intensity of β-chitin peaks (10° and 20°) was decreased in the case of nHAp incorporated composite scaffolds (Blackwell, 1969). The decrease in the intensity was due to the interaction of nHAp with β-chitin.

Thermogravimetric analysis of nHAp and composite scaffolds was performed at a linear rate of 10 °C/min from 25 to 500 °C in nitrogen atmosphere. In the TGA, nHAp does not undergo any change and the thermogram remains almost as a straight line. This is because of the high thermal stability of nHAp. The incorporation of nHAp did not alter the thermal stability of β-chitin. The initial dip at 50–100 °C in the thermograms was due to the evaporation of moisture content. All the scaffolds started degrading at 280 °C and 75% degradation occurred in β-chitin + 1% nHAp scaffold, 80% in β-chitin + 0.5% nHAp and 95% in β-chitin control at 500 °C. This was due to degradation of polysaccharide units of the polymer (Saito et al., 2000).

Differential thermal analysis of nHAp, β-chitin + 0.5% nHAp and β-chitin + 1% nHAp was performed. In the case of nHAp there was a broad exothermic peak between 200–320 °C; which was due to the crystallization of nHAp. The scaffolds degraded at higher temperature and the peaks at 370 and 470 °C correspond to this decomposition (refer Supplementary Data).

Fig. 2A shows the porosity of the prepared nanocomposite scaffolds. β-Chitin control scaffolds showed about 80% porosity whereas nHAp incorporated scaffolds indicated lesser porosity. This was due to the presence of nHAp throughout the scaffold which binds to the polymer chains and helps to hold the polymer chains of β-chitin intact. Porosity is an important factor for an ideal scaffold to be used in tissue engineering applications (Liuyun et al., 2009). Cells can travel through the pores and get attached at suitable positions in the scaffolds for further proliferation. So, for the prepared nanocomposite scaffolds the obtained porosity is sufficient and the porosity aids in the supply of nutrients and oxygen to the interior regions of the composite scaffolds.

Fig. 2B shows the swelling ratio of the control and composite scaffolds. The swelling ability of the scaffolds was evaluated up to 28 days. From the figure, it was clear that the incorporation of nHAp reduced the swelling capacity. This was owing to the reduction in total porosity of the composite scaffolds due to the presence of nHAp. The control scaffold showed a swelling ratio of 20 within 24 h in contact with the liquid. The 0.5 & 1% nHAp incorporated scaffolds showed a swelling ratio of 18 and 14, respectively. One important point to be noted here is that within 24 h itself the scaffolds were almost saturated. On 7th day, maximum swelling capacity has been attained and thereafter the swelling ratio trend was found to decrease. This was due to the rupture of polymer chains at higher stage of swelling. At 28th day, control scaffolds showed swelling ratio of 18 and composite scaffolds showed 14. The swelling ability of the scaffolds will help to absorb the culture medium and hence allow the easy passage of nutrients through it (Peter et al., 2010).

3.2. *In vitro degradation studies*

Fig. 2C shows the *in vitro* biodegradation data of the scaffolds. At day 7, around 10% of all the scaffolds was degraded. At higher duration of time, the rate of degradation was also increased. About 15–20% of degradation occurred at day 14. On completion of 28 days, control scaffold degraded 45% and nHAp incorporated scaffolds (0.5% and 1%) degraded 30%. Chitin can be degraded by lysozyme present in the human body. The degradation products can further help to attract more cells towards the scaffold and hence improve the bioactivity of the scaffolds. Controlled degradation is essential for an ideal scaffold for tissue engineering applications.

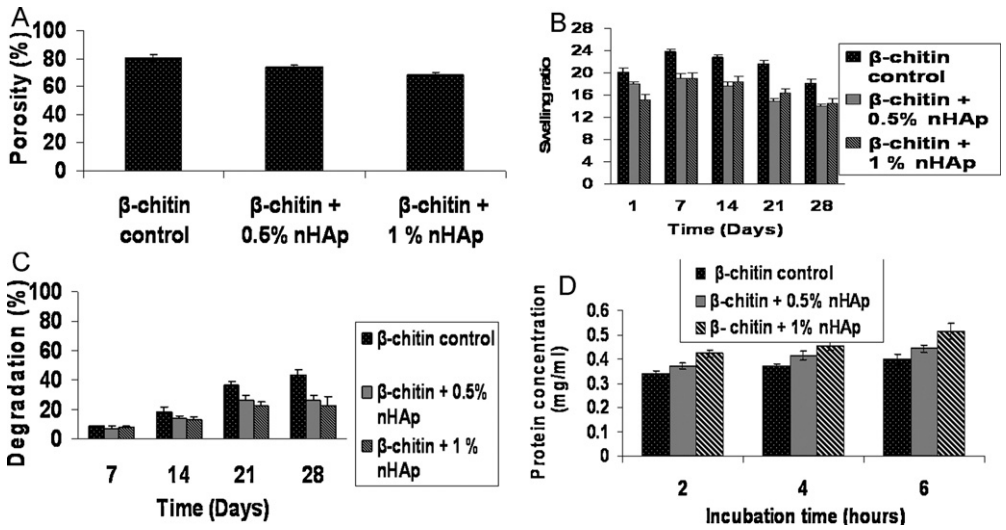

Fig. 2. (A) Porosity of scaffolds. (B) Swelling ratio of scaffolds. (C) Biodegradation of scaffolds. (D) Protein adsorption of control and composite scaffolds.

3.3. Protein adsorption study

Fig. 2D indicates the protein adsorption data of the scaffolds. Protein adsorption is known to influence the cell adhesion by adsorption of key adhesion molecules like fibronectin or vitronectin (Kim et al., 2005). The adsorbed protein concentration was increased with time from 2 to 6 h. The increase in protein adsorption on the β-chitin + 0.5% nHAp and β-chitin + 1% nHAp composite scaffolds than control scaffold can be due to the distribution of nHAp particles on the scaffold surfaces, which increases the binding sites on the material surface for proteins, or promotes an electrostatic interaction between the proteins and material surface and enhances adsorption of proteins (Wang et al., 2007).

3.4. In vitro biomineralization studies

Fig. 3 shows the SEM images of *in vitro* biomineralization studies of the scaffolds. A, B and C correspond to β-chitin control at 7, 14 and 21 days, respectively. Images D, E and F correspond to β-chitin + 0.5% nHAp at 7, 14 and 21 days, respectively. The images

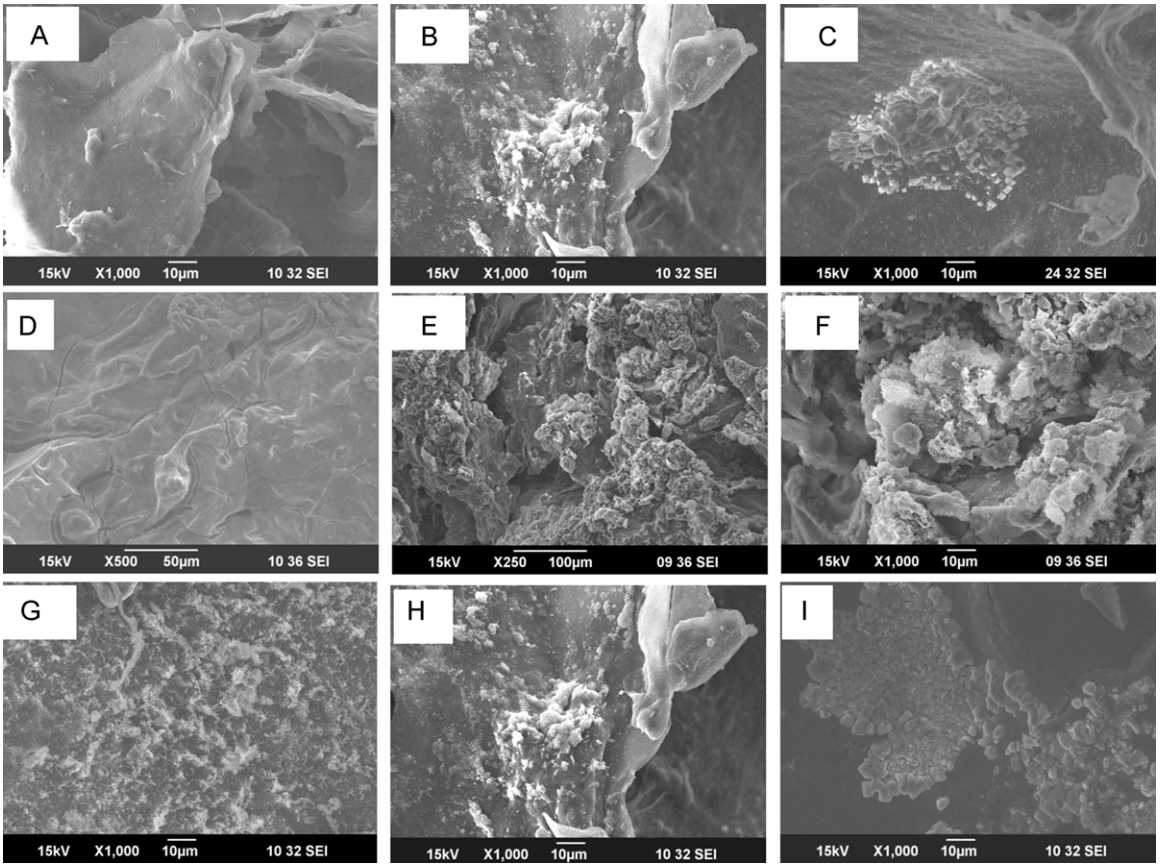

Fig. 3. SEM images of biomineralization. A, B and C correspond to β-chitin control at 7, 14 and 21 days, respectively. D, E and F correspond to β-chitin + 0.5% nHAp at 7, 14 & 21 days, respectively. G, H and I correspond to β-chitin + 1% nHAp at 7, 14 & 21 days, respectively.

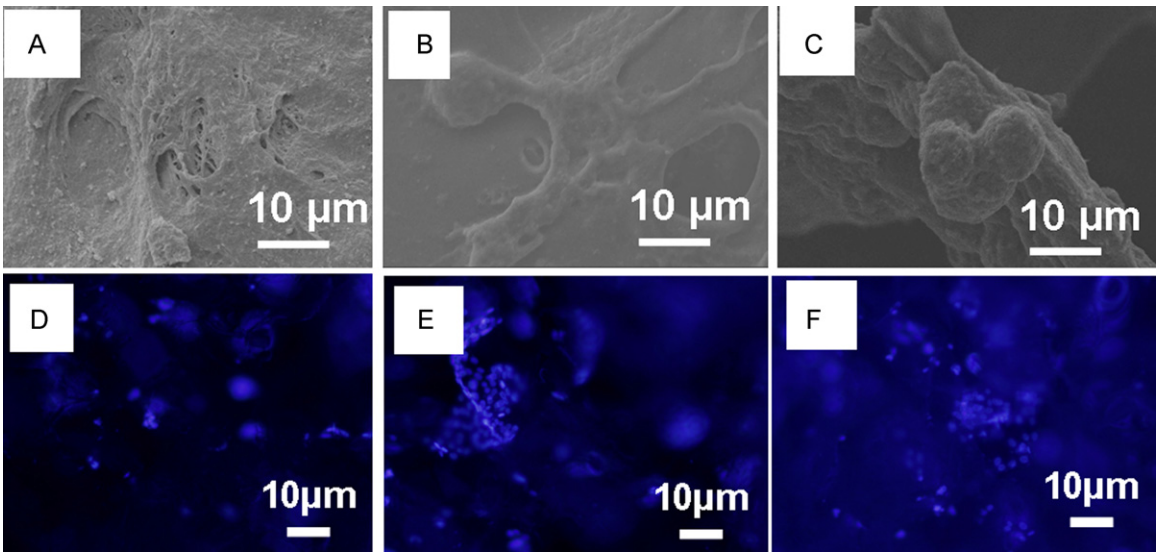

Fig. 4. SEM images of cell attachment and DAPI images with MG63. A, B and C are SEM images of cell attachment of β-chitin control, β-chitin + 0.5% nHAp and β-chitin + 1% nHAp scaffolds, respectively at 72 h and D, E & F are DAPI images of β-chitin control, β-chitin + 0.5% nHAp and β-chitin + 1% nHAp scaffolds, respectively at 72 h.

G, H and I correspond to β-chitin + 1% nHAp at 7, 14 and 21 days, respectively. The images showed an apatite layer deposition on the scaffold surfaces at day 7. At day 7, scaffolds containing nHAp showed more apatite layer deposition than control and at 14 and 21 days the density of the apatite layer was increased. This indicated that nHAp will initiate the cells to deposit more minerals and extracellular matrix on the surface of the scaffolds (Madhumathi et al., 2009). These results indicated that increasing the soaking time in SBF will enhance the apatite layer formation on the surface of the composite scaffolds. The presence of nHAp also plays a role in this enhanced apatite deposition.

The FT-IR spectra of biomineralization showed sharpening of peaks at 602 and 565 cm^{-1} corresponding to stretching vibration bands of phosphate group and at 3570 cm^{-1} attributed to OH group (Peter et al., 2010). The spectra indicate an increase in the intensity of peaks from 7 to 21 days (Katerina et al., 2010).

The XRD spectra of biomineralization showed a sharp peak at 25.8 and 31.5° (2θ) attributed to 2 1 1 plane of hydroxyapatite. The intensity of the peaks was found to increase from 7 to 21 days (Madhumathi et al., 2009).

All these data revealed the biomineralization capability of the composite scaffolds which will be helpful for the scaffolds for bone tissue engineering (refer Supplementary Data).

3.5. Cell viability

The cell viability of the composite scaffolds was analyzed by treating with MG63, Vero, NIH3T3 and HDF cells for 24 and 48 h. All cells showed almost 100% viability compared to the controls after 24 and 48 h of incubation. The presence of nHAp does not affect the cytocompatible nature of the scaffolds.

3.6. Cell attachment and proliferation studies

Figs. 4–7 correspond to the cell attachment and proliferation studies of MG63, Vero, NIH3T3 and HDF cells, respectively. In all these figures, A and D correspond to the SEM and DAPI images of cell attachment of β-chitin control at 72 h. Images B and E correspond to the SEM and DAPI images of cell attachment on the surfaces of the β-chitin + 0.5% nHAp scaffolds at 72 h. Images C and F represent

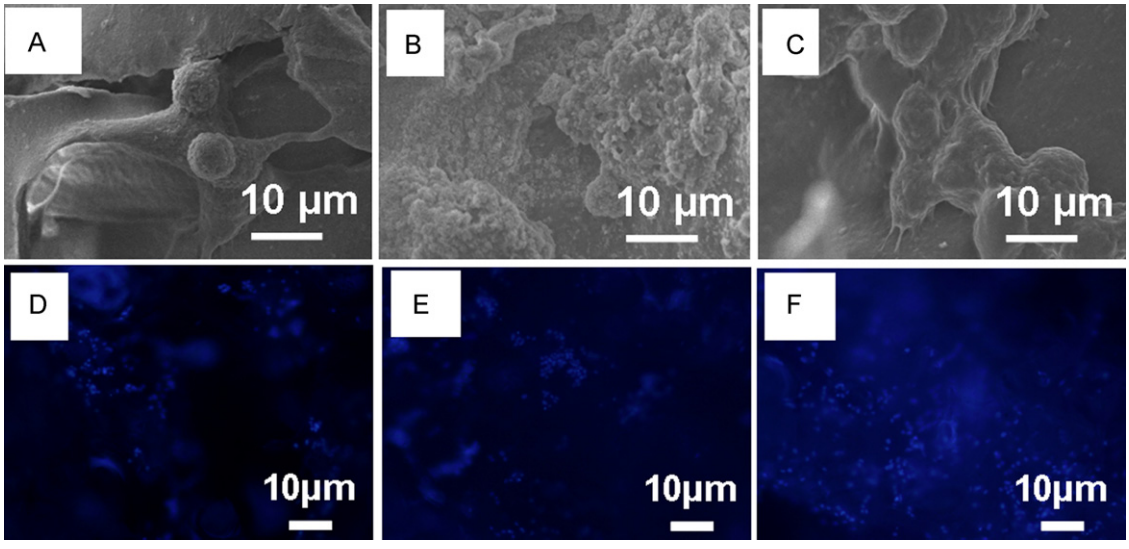

Fig. 5. SEM images of cell attachment and DAPI images with Vero. A, B and C are SEM images of cell attachment of β-chitin control, β-chitin + 0.5% nHAp and β-chitin + 1% nHAp scaffolds, respectively at 72 h and D, E and F are DAPI images of β-chitin control, β-chitin + 0.5% nHAp and β-chitin + 1% nHAp scaffolds, respectively at 72 h.

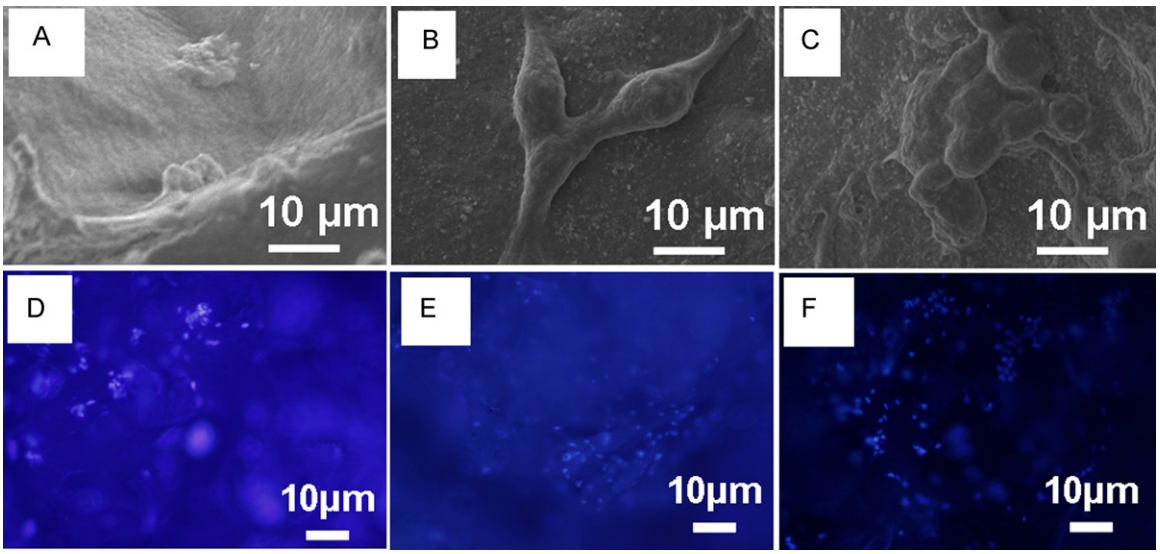

Fig. 6. SEM images of cell attachment and DAPI images of scaffolds with NIH3T3. A, B and C are SEM images of cell attachment of β-chitin control, β-chitin + 0.5% nHAp and β-chitin + 1% nHAp scaffolds, respectively at 72 h and D, E and F are DAPI images of β-chitin control, β-chitin + 0.5% nHAp and β-chitin + 1% nHAp scaffolds, respectively at 72 h.

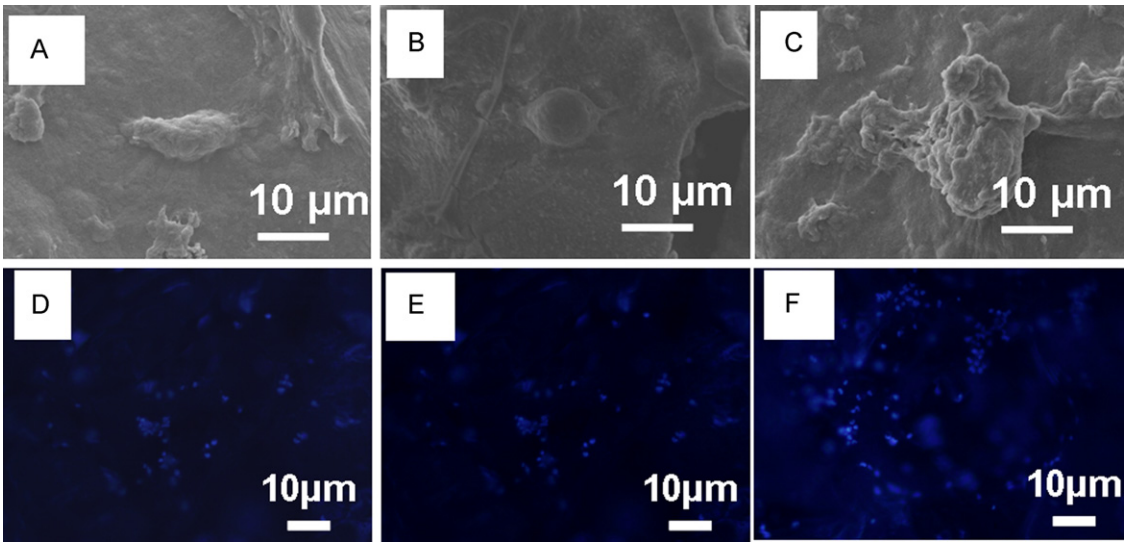

Fig. 7. Cell attachment and DAPI images of scaffolds with HDF. A, B & C are SEM images of cell attachment of β-chitin control, β-chitin + 0.5% nHAp and β-chitin + 1% nHAp scaffolds, respectively at 72 h and D, E & F are DAPI images of β-*chitin control*, β-chitin + 0.5% nHAp and β-chitin + 1% nHAp composite scaffolds, respectively at 72 h.

the SEM and DAPI images of cell attachment, respectively on the surfaces of the β-chitin + 1% nHAp composite scaffolds.

The SEM images showed that more number of cells were attached on the surface of the nHAp incorporated scaffolds than the control scaffold and the rounded morphology of the cells was clearly seen in the case of control at 12 h; whereas cells were evenly attached and spread throughout the nHAp incorporated scaffolds. At 72 h of study, it was found that the cells proliferated throughout the scaffolds. This was due to the presence of nHAp in the scaffolds which will help to adsorb more proteins on the scaffold surfaces. These adsorbed proteins will attract more number of cells towards those regions and hence will enhance the attachment and proliferation.

Fluorescent images of DAPI staining of cells incubated for 12 h and 72 h on the composite scaffolds also revealed that cells were attached and distributed throughout the scaffold. More cells were found to be attached on the β-chitin + 1% nHAp and β-chitin + 0.5% nHAp composite scaffolds than in β-chitin control scaffolds. These data indicate that the composite scaffolds showed enhanced biocompatibility than the control scaffolds.

4. Conclusions

β-Chitin hydrogel/nHAp composite scaffolds were synthesized from the hydrogel of β-chitin with nHAp. The prepared nanocomposite scaffolds showed well interconnected microporous structure (300–400 μm) and controlled swelling ratio in the range of 15–20. The incorporation of nHAp helped to attained controlled degradation and adequate protein adsorption. The incorporation of nHAp also enhanced the biomineralization of the nanocomposite scaffolds. Cell viability studies were performed using Vero, NIH3T3, MG63 and HDF cells which proved the cytocompatibility and well distributed pattern throughout the nanocomposite scaffolds and can be used for bone and wound tissue engineering.

Acknowledgments

One of the authors *R. Jayakumar* is grateful to SERC Division, Department of Science and Technology (DST), India, for providing the fund under the scheme of "Fast Track Scheme for Young Investigators" (Ref. No. SR/FT/CS-005/2008). *Dr. S. V. Nair* also grateful to DST, India, which partially supported this work, under a center grant of the Nanoscience and Nanotechnology Initiative program monitored by *Dr. C.N.R. Rao*. The authors are also thankful to *Mr. Sajin P. Ravi* for his help in SEM studies.

Appendix A. Supplementary data

Supplementary data associated with this article can be found, in the online version, at doi:10.1016/j.carbpol.2011.03.018.

References

Binulal, N. S., Deepthy, M., Selvamurugan, N., Shalumon, K. T., Suja, S., Mony, U., et al. (2010). Role of nanofibrous poly(caprolactone) scaffolds in human mesenchymal stem cell attachment and spreading for in bone tissue engineering – response to osteogenic regulators. *Tissue Engineering: Part A*, *16*, 393–404.

Blackwell, J. (1969). Structure of β-chitin or parallel chain systems of poly-β-(1 → 4)-N-acetyl-D-glucosamine. *Biopolymers*, *7*, 281–289.

Bonfield, W., Grynpas, M. D., Tully, A. E., & Bowman, A. J. (1981). Hydroxyapatite reinforced polyethylene a mechanically compatible implant material for bone replacement. *Biomaterials*, *2*, 185–196.

Chai, C., Nissan, B. B., Pyke, S., & Evans, L. (1995). Sol gel derived hydroxyapatite coatings for biomedical applications. *Materials and Manufacturing Processes*, *10*, 205–216.

Gkioni, K., Leeuwenburgh, S. C. G., Douglas, T. E. L., Mikos, A. G., & Jansen, J. A. (2010). Mineralization of hydrogels for bone regeneration. *Tissue Engineering: Part B*, *16*, 577–585.

Heise, U., Osborn, J. F., & Duwe, F. (1990). Hydroxyapatite ceramic as a bone substitute. *International Orthopaedics*, *14*, 329–338.

Jang, M. K., Kong, B. G., Jeong, Y., Lee, C. H., & Nah, J. W. (2004). Physicochemical characterization of α-chitin, β-chitin and γ-chitin separated from natural resources. *Journal of Polymer Science Part A: Polymer Chemistry*, *42*, 3423–3432.

Jayakumar, R., Prabaharan, M., Sudheesh, K. P. T., Nair, S. V., & Tamura, H. (2011). Biomaterials based on chitin and chitosan in wound dressing applications. *Biotechnology Advances*, *29*, 322–327.

Kim, H. W., Jonathan, C. K., & Hyoun, E. E. K. (2005). Hydroxyapatite porous scaffold engineered with biological polymer hybrid coating for antibiotic Vancomycin release. *Journal of Material Science Materials in Medicine*, *16*, 189–195.

Kokubo, T., & Takadama, H. (2006). How useful is SBF in predicting in-vivo bone activity? *Biomaterials*, *27*, 2907–2915.

Labella, R., Bradena, M., & Deb, S. (1994). Novel hydroxyapatite-based dental composites. *Biomaterials*, *15*, 1197–1200.

Lavall, R. L., Assis, O. B. G., & Filho, S. P. C. (2007). β-Chitin from the pens of Loligo sp: Extraction and characterization. *Bioresource Technology*, *98*, 2465–2472.

Liuyun, J., Yubao, L., & Chengdong, X. (2009). Preparation and biological properties of a novel composite scaffold of nano-hydroxyapatite/chitosan/carboxymethyl cellulose for bone tissue engineering. *Journal of Biomedical Science*, *16*, 65–74.

Madhumathi, K., Binulal, N. S., Nagahama, H., Tamura, H., Shalumon, K. T., Selvamurugan, N., et al. (2009). Preparation and characterization of novel β-chitin-hydroxyapatite composite membranes for tissue engineering applications. *International Journal of Biological Macromolecules*, *44*, 1–5.

Maeda, Y., Jayakumar, R., Nagahama, H., Furuike, T., & Tamura, H. (2008). Synthesis, characterization and bioactivity studies of novel β-chitin scaffolds for tissue-engineering applications. *International Journal of Biological Macromolecules*, *42*, 463–467.

Muzzarelli, R. A. A. (2009). Chitins and chitosans for the repair of wounded skin, nerve, cartilage and bone. *Carbohydrate Polymers*, *76*, 167–182.

Muzzarelli, R. A. A. (2011). Chitosan composites with inorganics, morphogenetic proteins and stem cells, for bone regeneration. *Carbohydrate Polymers*, *83*, 1433–1445.

Nagahama, H., Kashiki, T., Nwe, N., Jayakumar, R., Furuike, T., & Tamura, H. (2008). Preparation of biodegradable chitin/gelatin membranes with GlcNAc for tissue engineering applications. *Carbohydrate Polymers*, *73*, 456–463.

Nguyen, K. T., & West, J. L. (2002). Photopolymerizable hydrogels for tissue engineering applications. *Biomaterials*, *23*, 4307–4314.

Peesan, M., Rujiravanit, R., & Supaphol, P. (2003). Characterization of β-chitin/poly(vinyl alcohol) blend films. *Polymer Testing*, *22*, 381–387.

Peter, M., Nitya, G., Selvamurugan, N., Nair, S. V., Furuike, T., Tamura, H., et al. (2010). Preparation and characterization of chitosan-gelatin/nanohydroxyapatite composite scaffolds for tissue engineering applications. *Carbohydrate Polymers*, *80*, 687–694.

Rashidova, S. S., Milusheva, R. Y., Voropaeva, N. L., Pulatova, S. R., Nikonovich, G. V., & Ruban, I. N. (2004). Isolation of chitin from a variety of raw materials, modification of the material, and interaction its derivatives with metal ions. *Chromatographia*, *59*, 783–786.

Rudall, K., & Kenchington, M. W. (1973). The chitin system. *Biological Reviews*, *48*, 597–633.

Saito, Y., Okano, T., Gaill, F., Chanzy, H., & Putaux, J. C. (2000). Structural data on the intra-crystalline swelling of β-chitin. *International Journal of Biological Macromolecules*, *28*, 81–88.

Sudheesh, K. P. T., Abhilash, S., Manzoor, K., Nair, S. V., Tamura, H., & Jayakumar, R. (2010). Preparation and characterization of novel β-chitin/nanosilver composite scaffolds for wound dressing applications. *Carbohydrate Polymers*, *80*, 761–767.

Sugiyama, J., Boisset, C., & Hashimoto, M. (1999). Molecular directionality of β-chitin biosynthesis. *Journal of Molecular Biology*, *286*, 247–255.

Tamura, H., Furuike, T., Nair, S. V., & Jayakumar, R. (2011). Biomedical applications of chitin hydrogel membranes and scaffolds. *Carbohydrate Polymers*, *84*, 821–825.

Tamura, H., Nagahama, H., & Tokura, S. (2006). Preparation of chitin hydrogel under mild conditions. *Cellulose*, *13*, 357–364.

Tan, H., & Marra, K. G. (2010). Injectable, biodegradable hydrogels for tissue engineering applications. *Materials*, *3*, 1746–1767.

Verheyen, C. C., Dewijn, J. R., van Blitterswijk, C. A., & de Groot, K. (1992). Evaluation of hydroxyapatite/poly(L-lactide) composites: Mechanical behavior. *Journal of Biomedical Materials Research*, *26*, 1277–1296.

Wang, H. N., Li, Y. B., Zuo, Y., Li, J. H., Ma, S. S., & Cheng, L. (2007). Biocompatibility and osteogenesis of biomimetic nano-hydroxyapatite/polyamide composite scaffolds for bone tissue engineering. *Biomaterials*, *28*, 3338–4334.

Wang, X., Li, Y., Wei, J., & Groot, K. (2002). Development of biomimetic nano-hydroxyapatite/poly (hexamethylene adipamide) composites. *Biomaterials*, *23*, 4787–4791.